List of Figures

List of Tables

Figure S1

The complete flow diagram of the mechanism from preparing the ingot (Pt-Ce) to atmosphere-treated Pt-Ce film depicts a 3-step pattern emergence based on phase separation.

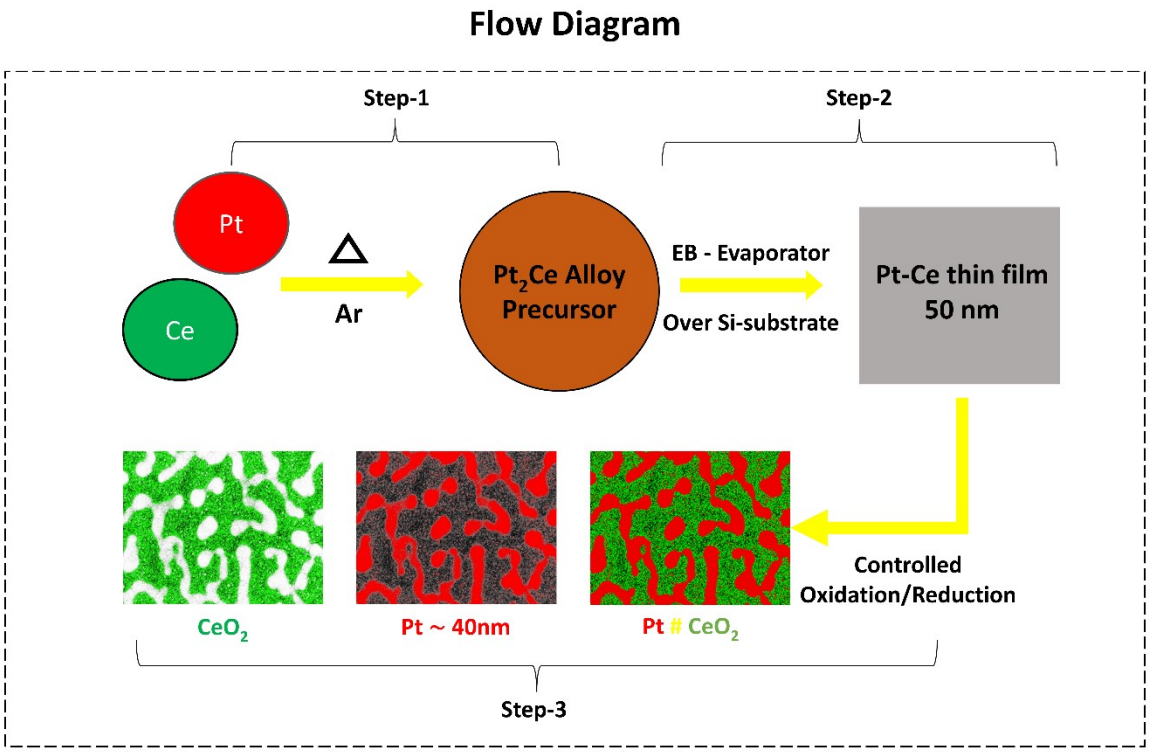

Figure 1. The complete flow diagram of the mechanism

Figure S2

FE-SEM image of the atmosphere-treated Pt-Ce film, which is shown in Figure 1 of the article.

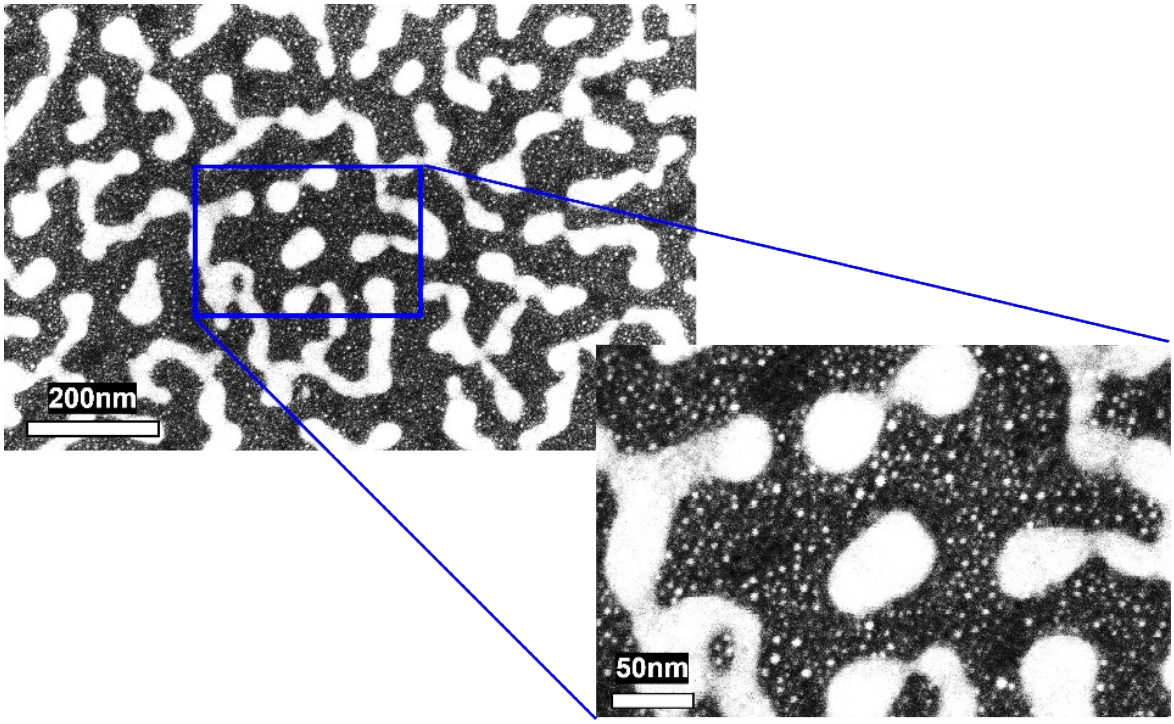

Figure 2. Corresponding FE-SEM image of Figure 1 of the manuscript

Figure S3

*p*XRD data of the as-prepared ingot of Pt-Ce. Showing clear peaks from Pt-Ce alloy matching the referred Powder Diffraction File (PDF) taken from The International Centre for Diffraction Data ICDD database.

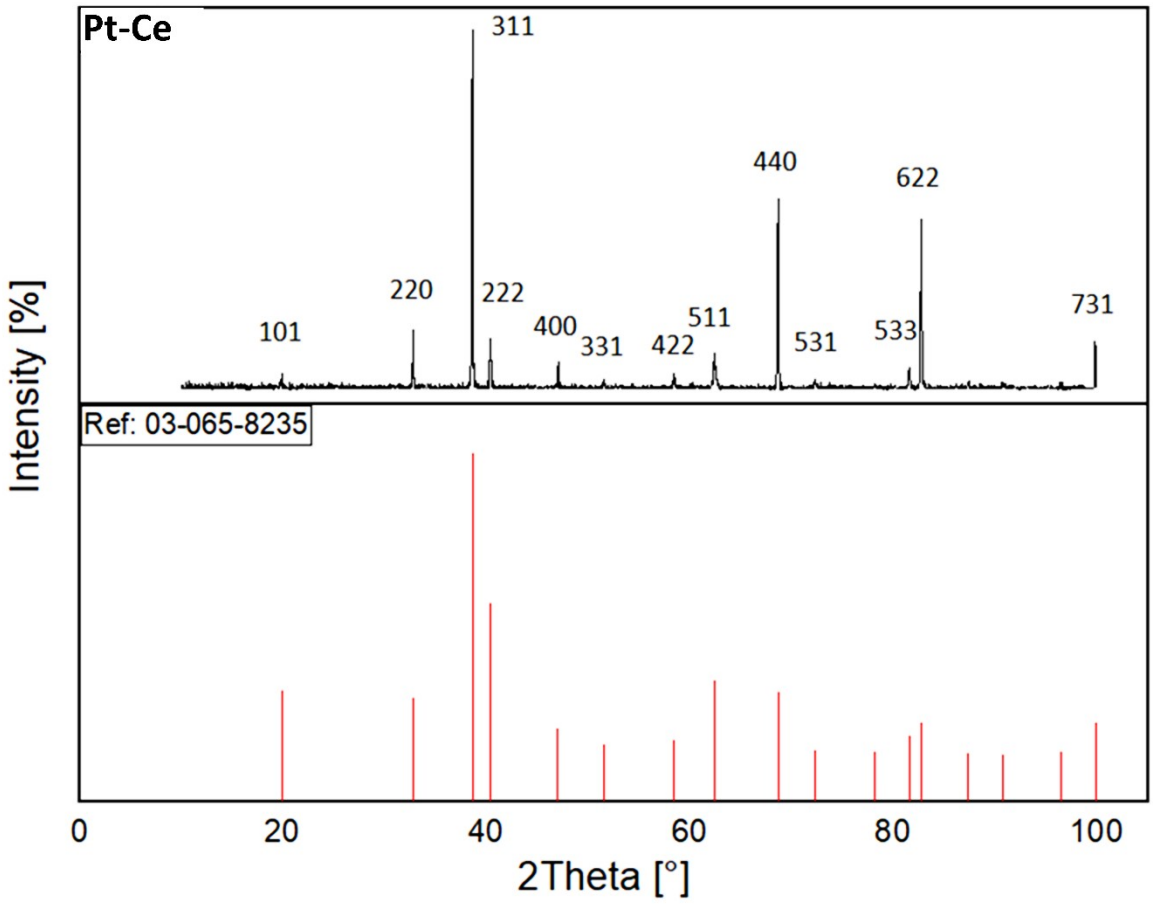

Figure 3. pXRD data of the as-prepared ingot Pt-Ce

Figure S4

FE-SEM images of an as-deposited Pt-Ce film. The film even at the scale of 50nm looks very uniform and evenly distributed.

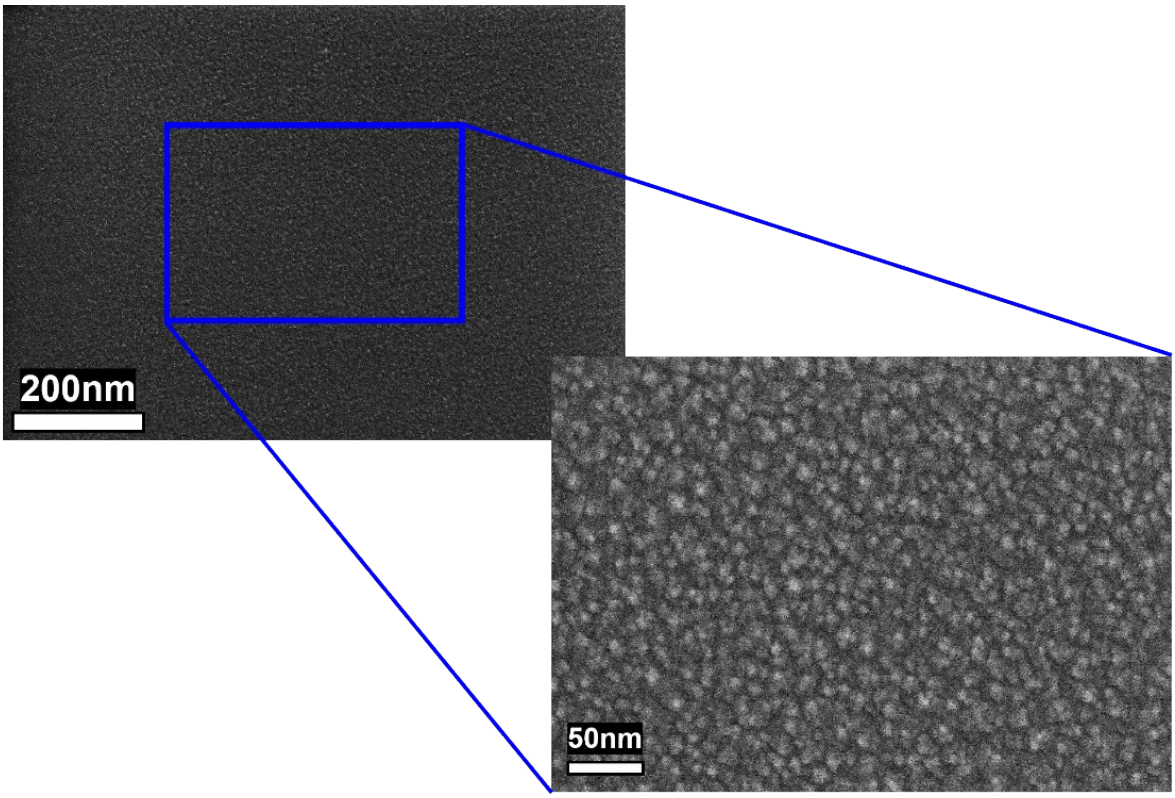

Figure 4. FE-SEM images of the as-deposited film (Pt-Ce).

Figure S5

(a) AFM image of an as-deposited Pt-Ce film. (b) Gives a 3D look of the AFM image to distinguish between different heights clearly. Confirms the smoothness as well as the uniformity of our as-deposited film. (c) KPFM image of the as-deposited film (Pt-Ce). Shows the uniform voltage profile, and also confirms the uniformity and smoothness of our as-deposited film. (d) AFM (black) and KPFM (red) height profiles are given for the as-deposited film (Pt-Ce). Both profiles show differences of around 3-4 nm between the highest signal and lowest single, showing how uniformly the deposition has been acquired.

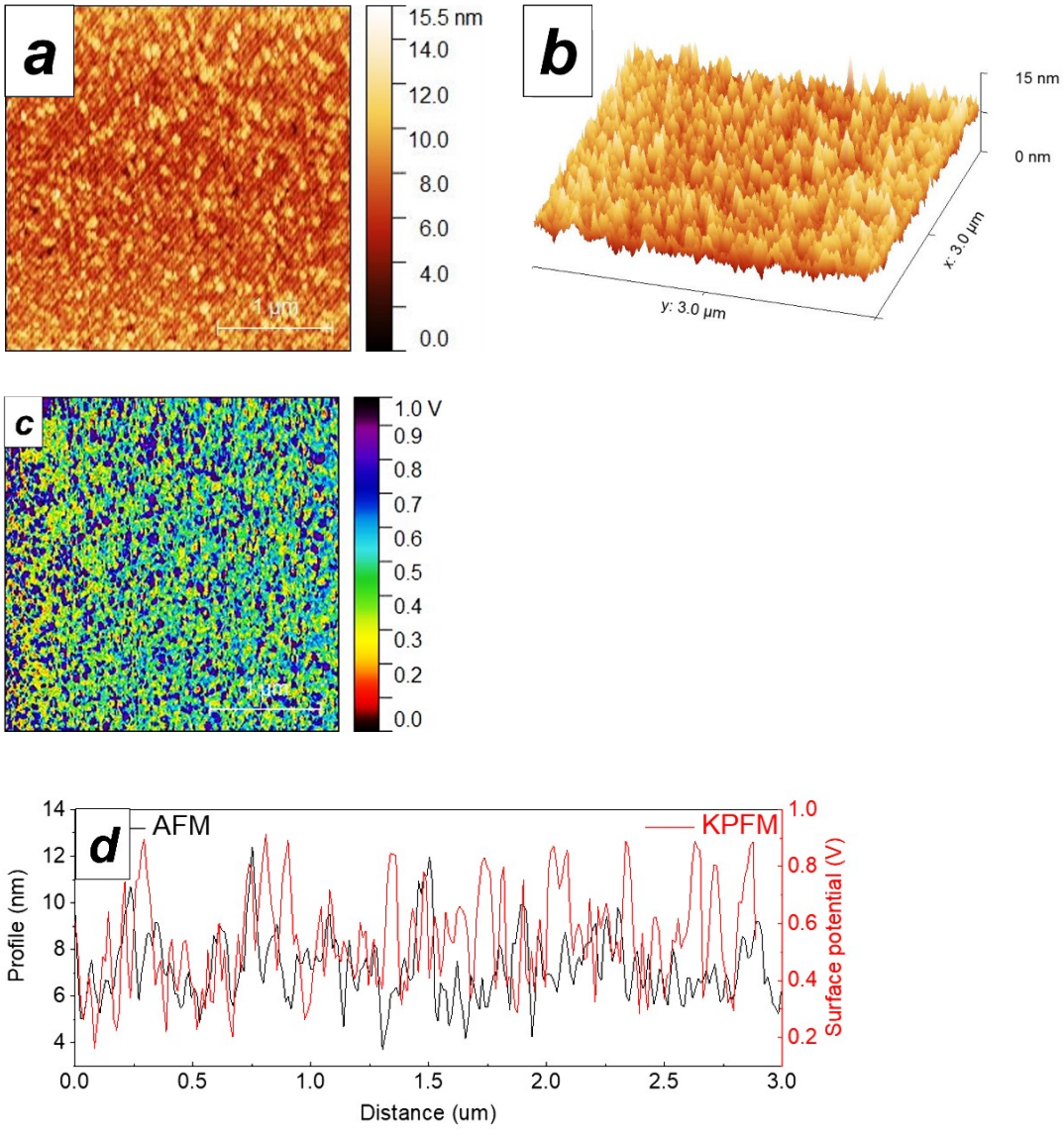

Figure 5. AFM, KPFM, and Height profile of the as-deposited film (Pt-Ce).

Figure S6

Shows the stability of the as-deposited Pt-Ce film, when subjected to pure argon atmosphere at 600^{o}C for 1 hour.

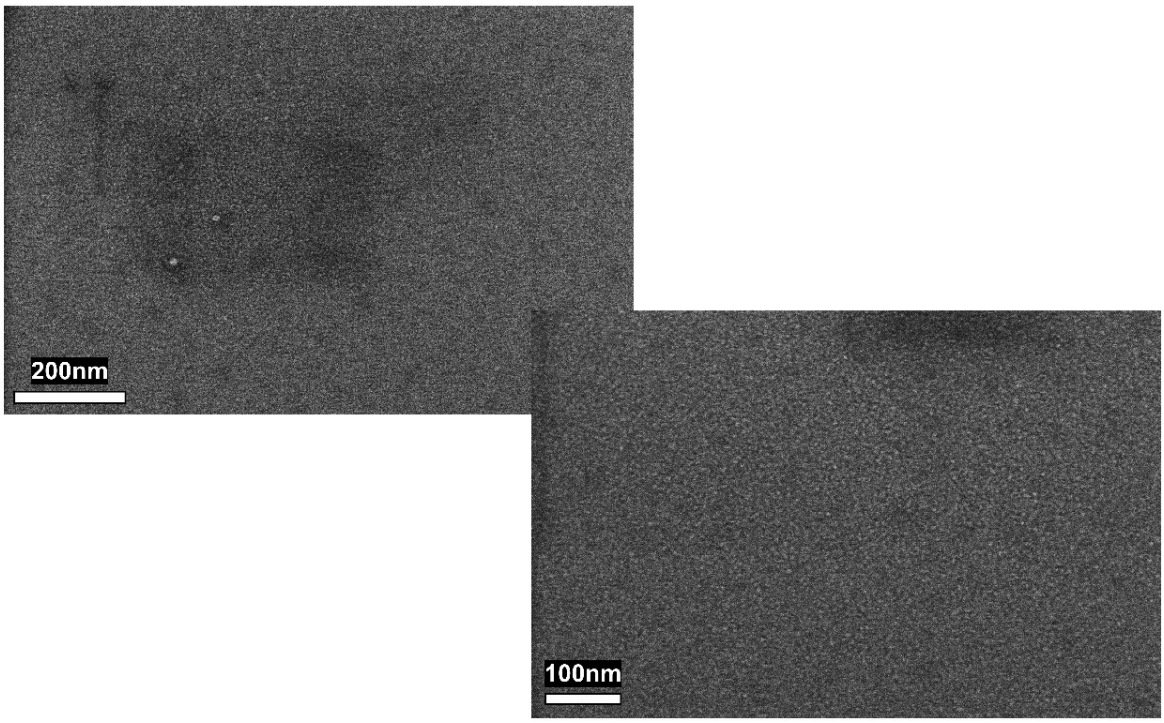

Figure 6. FE-SEM image of pure Argon-atmosphere treated as-deposited Pt-Ce film.

Figure S7

EDX-Mapping shows the existence of a homogeneous mixture of platinum (Pt) and cerium (Ce) components in the as-deposited Pt-Ce thin film, proving the uniform distribution.

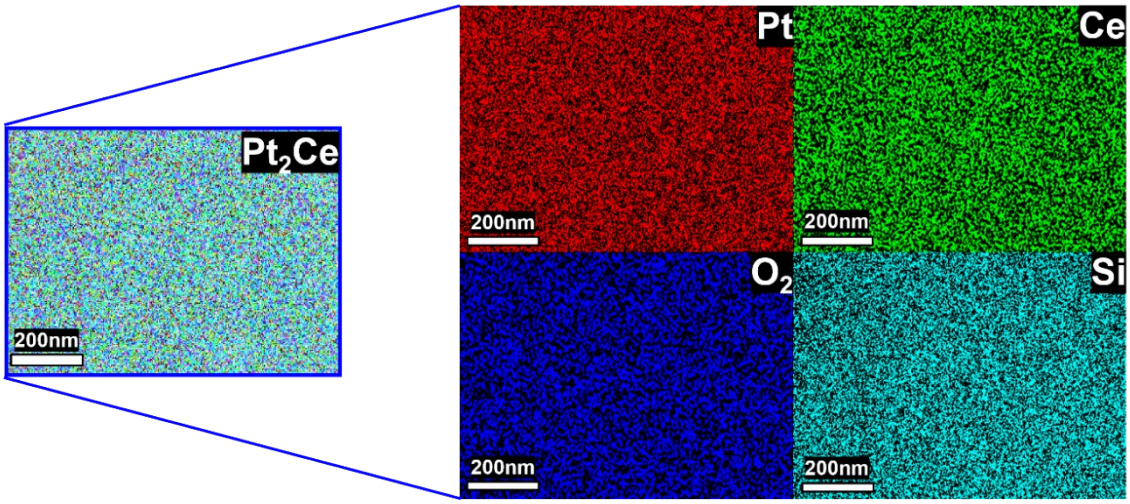

Figure 7. EDX-Mapping of the as-deposited Pt-Ce film.

Figure S8

EDX-Spectrum of our as-deposited film (Pt-Ce). The presence of the strong peaks from Pt and Ce atoms indicates purity in our Pt-Ce 2D film as well.

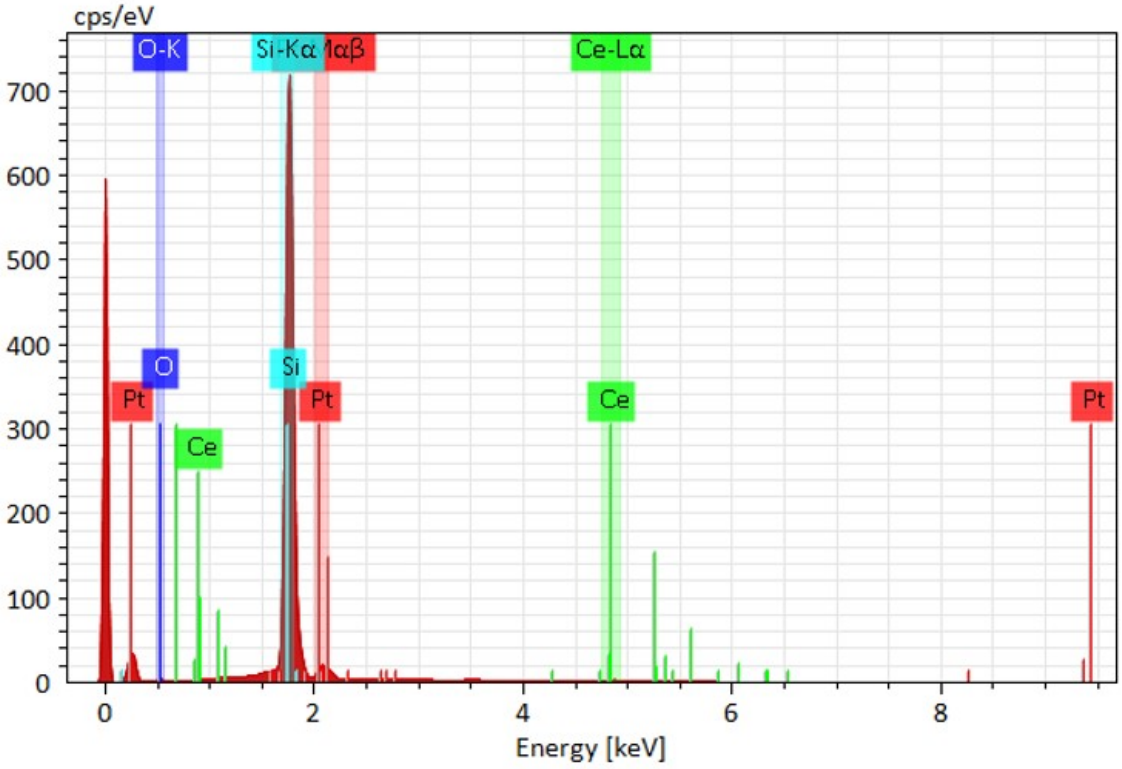

Figure 8. EDX-Spectrum of the as-deposited film (Pt-Ce)

Table S9

EDX-Quantitative analysis of the as-deposited 2D thin film (Pt-Ce). The approximate ratio is 1.95 ± 0.05.

Table 1. EDX-Quantitative analysis of the as-deposited (Pt-Ce) thin film.

Element	Weight%	Atomic%
O K	12.56	61.32
Ce L	23.47	13.08
Pt M	63.97	25.60
Totals	100.00	

Figure S10

A view of the atmosphere-treated Pt-Ce film confirms the uniform distribution of the pattern over the entire surface of the specimen.

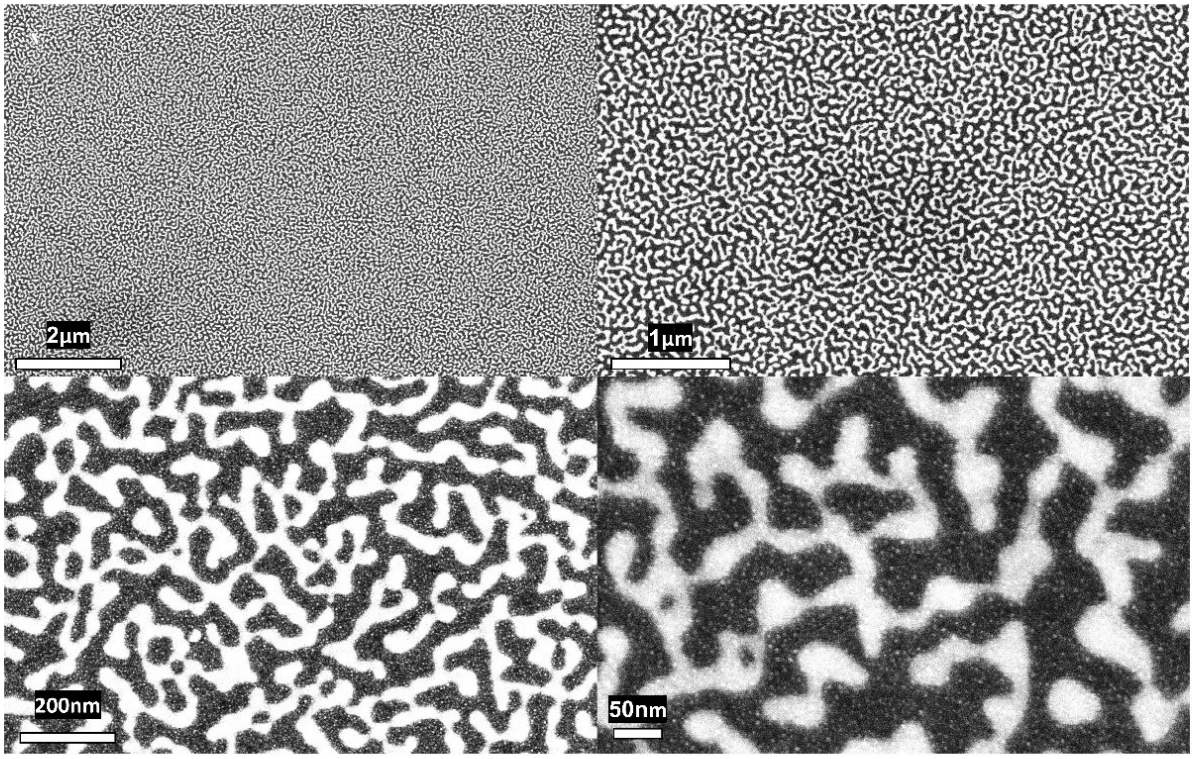

Figure 9. FE-SEM images of the post-treated Pt-Ce film at different magnifications.

Figure S11

Corresponding FE-SEM images of the atmosphere-treated Pt-Ce film, are shown in Figure 3(c) of the main article.

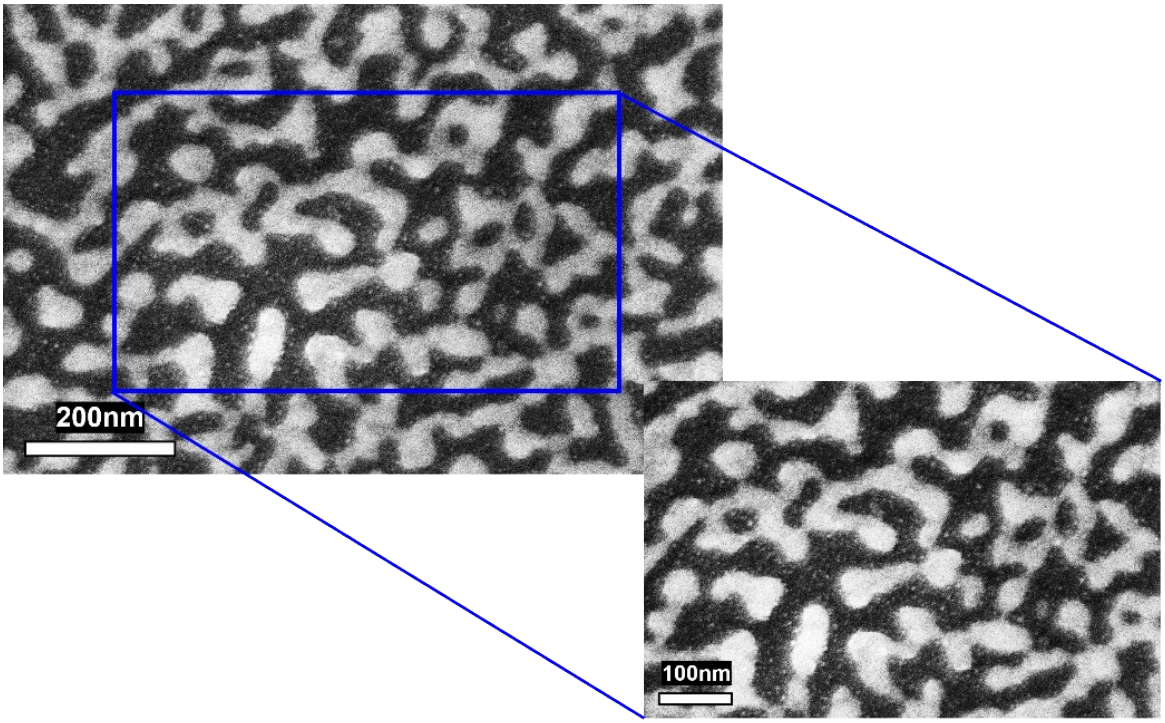

Figure 10. Corresponding FE-SEM images of Figure 3(c) of the main article.

Figure S12

EDX-Spectrum of the atmosphere-treated Pt-Ce film. Shows peaks from the individual Pt and Ce phases. Providing evidence of the composition of our post-treated film.

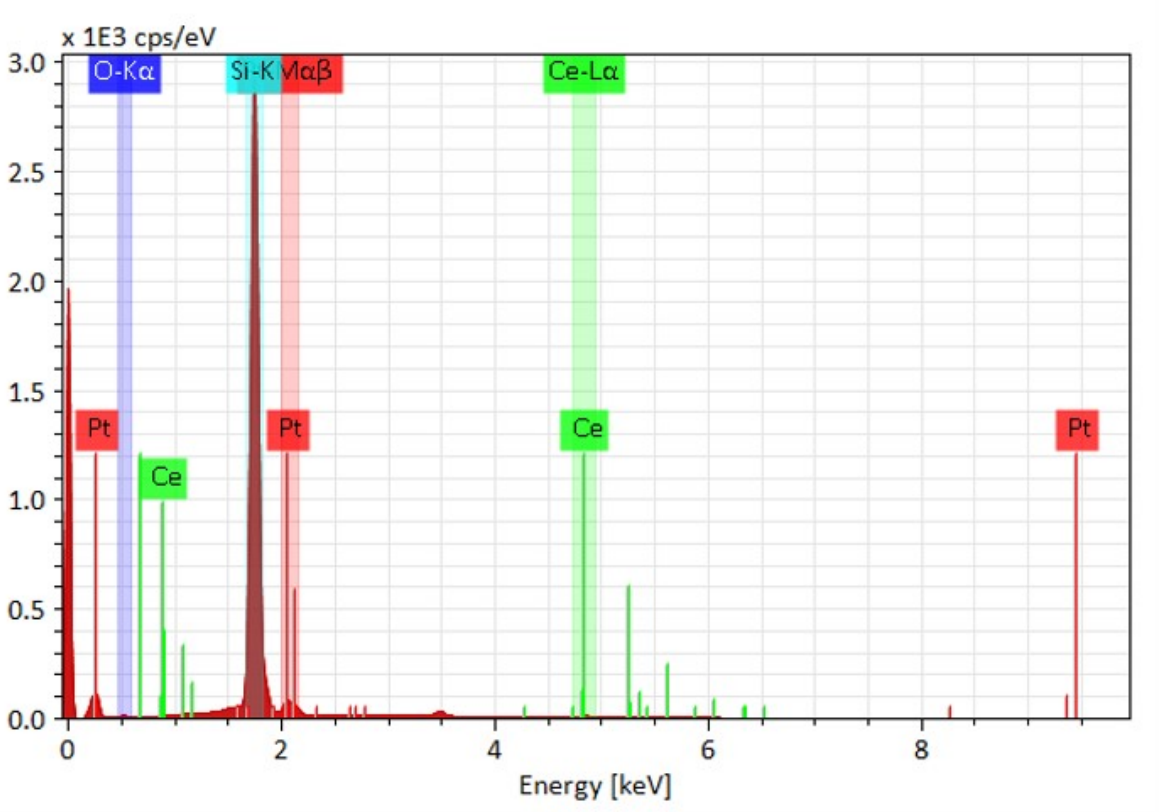

Figure 11. EDX-Spectrum of the atmosphere-treated Pt-Ce film.

Table S13

EDX-Quantitative analysis of the atmosphere-treated Pt-Ce film. The approximate ratio is Pt/Ce = 1.86 ± 0.05.

Table 2. EDX-Quantitative analysis of the atmosphere-treated Pt-Ce film.

Element	Weight%	Atomic%
O K	16.36	68.25
Ce L	23.33	11.11
Pt M	60.32	20.64
Totals	100.00	

Figure S14

A pair of gold-titanium (Au-Ti) terminals were deposited onto the post-treated film surface, maintaining a terminal gap of 25 µm with the help of an Aluminum wire having a thickness of 25 µm.

For the deposition of the terminals, electron beam evaporator (UEP-3000BS) was utilized. Firstly, the adhesion layer, containing Titanium (Ti) thin layer of 10 nm was deposited over the post-treated specimen at a very high vacuum level of 10^{-4} Pa. Then the Gold (Au) thin layer of 200nm was deposited over it as an electrode. The separation of 20-25 µm was maintained by using an Aluminum wire having an average thickness of 25 µm.

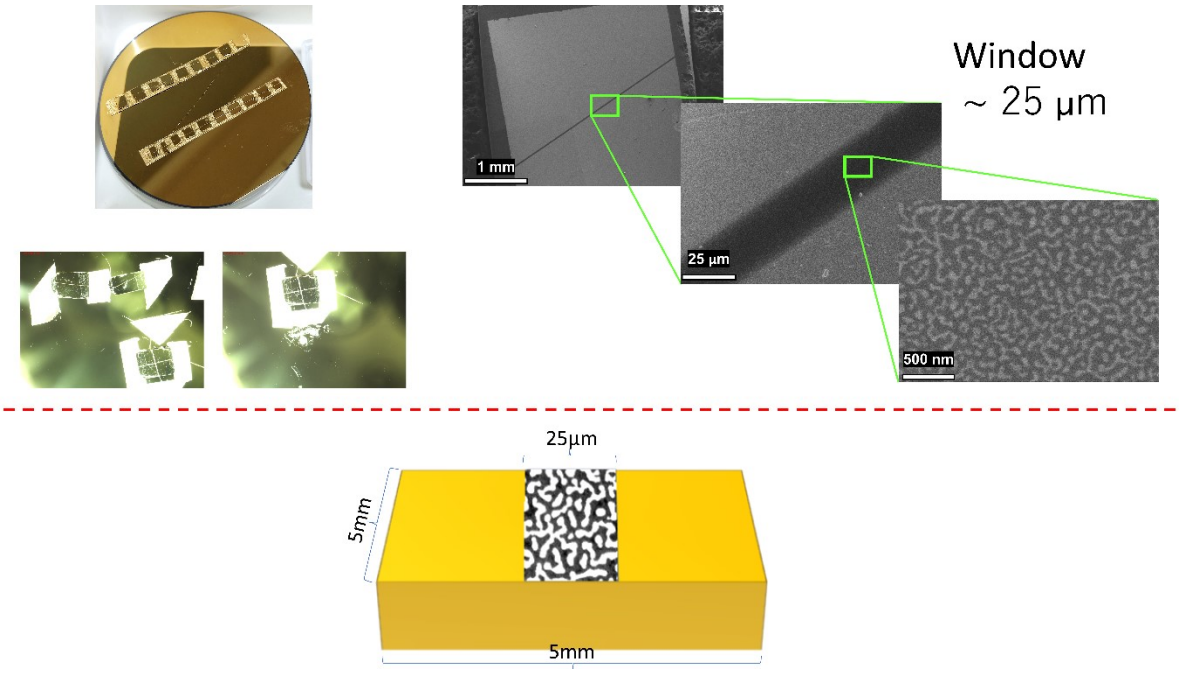

Figure 12. Au-Ti two terminal electrodes deposition procedure.

Figure S15

Two-terminal method setup for electrical resistance measurements. And the developed chemo-electric functionality measurement system on the right.

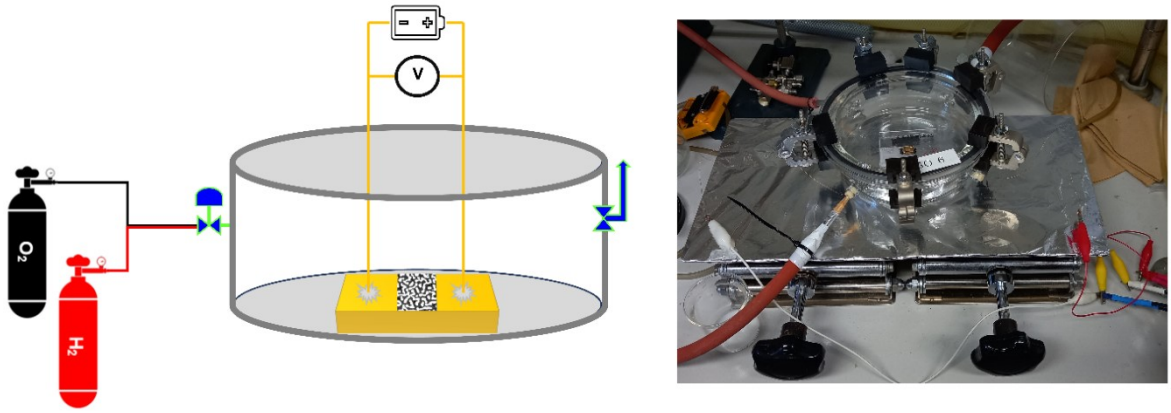

Figure 13. Two terminal electrical resistance measurement setups.

Table S16

Depicts the values gathered via using EC-Lab software corresponding to the graph in Fig. 5(c) of the article. The sky-blue color value represents Nitrogen gas and the corresponding resistance of our Pt nanonetworks in the presence of pure Nitrogen gas. Grey color values represent Oxygen gas and the corresponding resistance of our Pt nanonetworks in the presence of pure Oxygen gas. Red color values represent Hydrogen gas and the corresponding resistance of our Pt nanonetworks in the presence of pure Hydrogen gas.

Table 3. Depicts the measured resistances through EC-Lab software corresponding to the graph in Fig. 5(c) of the article.

Gas	Resistance (Ω)	Time (Mins)
N2	32.56	0
O2	33.36	5
H2	32.59	10
O2	33.34	15
H2	32.61	20
O2	33.35	25
H2	32.62	30
O2	33.34	35
H2	32.63	40
O2	33.34	45
H2	32.63	50
O2	33.34	55

Figure S17

Illustrates the schematic diagram of the mechanism behind our Pt nanonetwork's H_2 gas sensing.

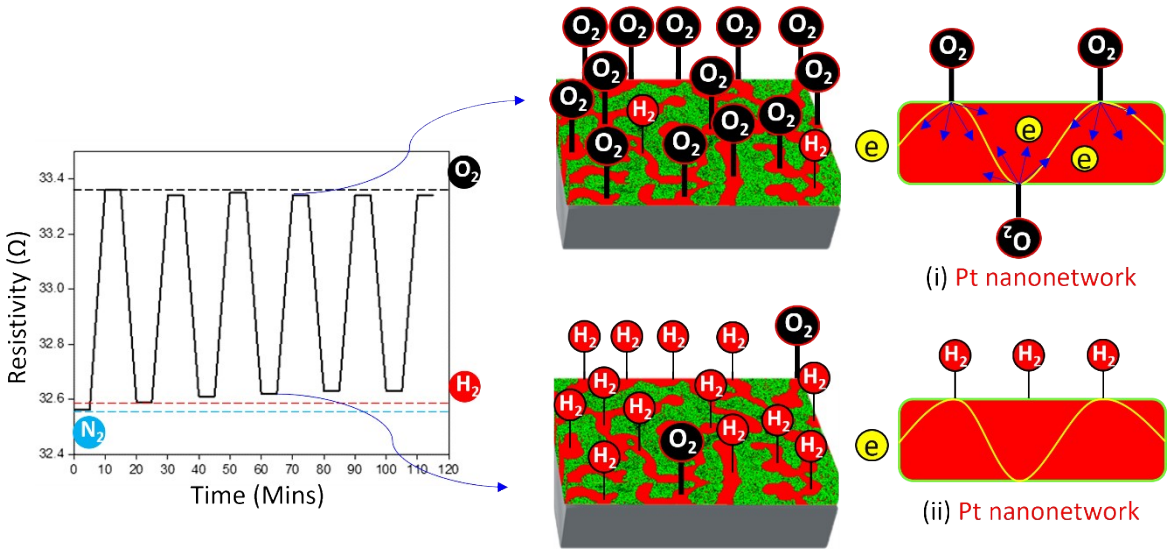

Figure 14. The schematic diagram of the H_2 gas sensing mechanism.

Figure S18

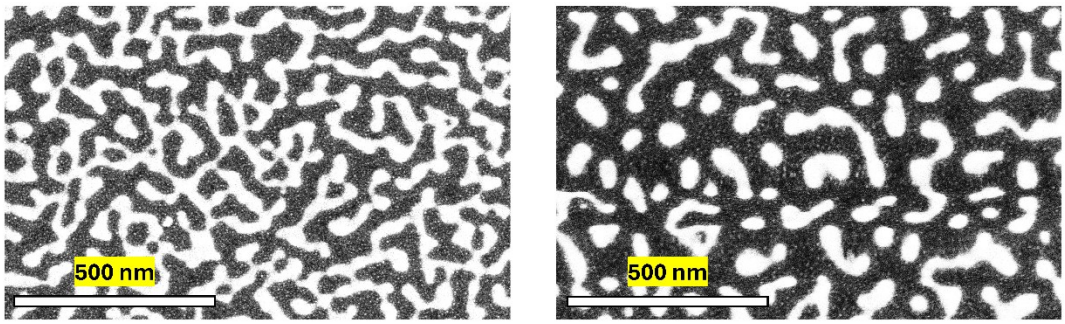

Figure 15. Post-treatment at different temperatures (a) shows a pattern at 600°C for 1 minute (b) shows a pattern at 700°C for 1 minute.

Table S19

Table 4 Shows H2 and N2 sensing mechanisms at different dilution ratios.

Set of readings	Gases		% Diluted		Resistance (Ω)	Time (Min)
1.	N_2	H_2	100%	0%	216.8	20
	N_2	H_2	99%	1%	217.2	10
2.	N_2	H_2	100%	0%	216.9	20
	N_2	H_2	90%	10%	217.3	10
3.	N_2	H_2	100%	0%	217.0	20
	N_2	H_2	50%	50%	217.4	10

Figure S20

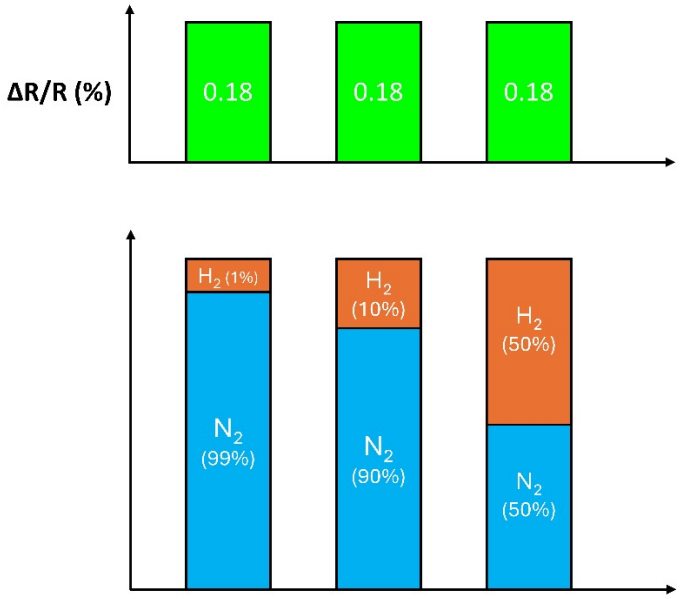

Figure 16. Illustrates the sensing capabilities of the reported sensor head at different concentrations of H_2

Table S21

Table 5. Shows H_2 and CH_4 sensing mechanisms at different dilution ratios.

Set of readings	Gases		% Diluted		Resistance (Ω)	Time (Min)
1.	N_2	CH_4	100%	0%	226.3	20
	N_2	CH_4	99%	1%	226.3	10
2.	N_2	CH_4	100%	0%	226.2	20
	N_2	CH_4	90%	10%	226.2	10
3.	N_2	CH_4	100%	0%	226.4	20
	N_2	CH_4	50%	50%	226.4	10

Figure S22

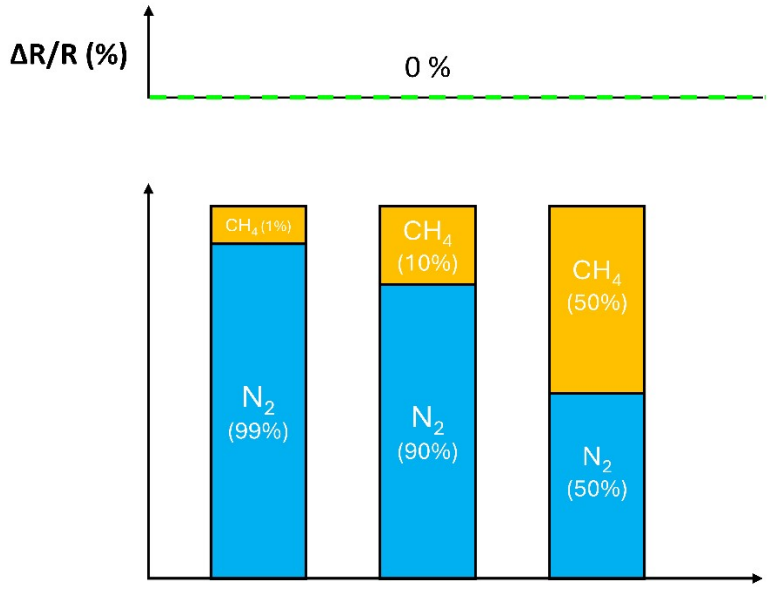

Figure 17. Illustrates the no sensing capabilities of the reported sensor head at different concentrations of CH_4